Songklanakarin J. Sci. Technol.
42 (1), 188-195, Jan. - Feb. 2020

http://www.sjst.psu.ac.th

Original Article

Improving telmisartan mechanical properties through the formation of telmisartan and oxalic acid co-crystal by slow evaporation and ultrasound assisted co-crystallization from solution methods

Hestiary Ratih[1, 2*], Jessie Sofia Pamudji[1], Fikri Alatas[2], and Sundani Nurono Soewandhi[1]

[1] *Pharmaceutics Group, School of Pharmacy, Bandung Institute of Technology, Kota Bandung, Jawa Barat, 40132 Indonesia*

[2] *Pharmaceutics Group, Faculty of Pharmacy, University of Jenderal Achmad Yani, Kota Cimahi, Jawa Barat, 40531 Indonesia*

Received: 16 April 2018; Revised: 2 September 2018; Accepted: 2 November 2018

Abstract

Telmisartan (TMS) is used for the prevention and treatment of hypertension. However, it has poor mechanical properties. The purpose of this research was to improve the mechanical properties of TMS through the formation of co-crystal TMS with oxalic acid (OXA) and to compare the mechanical properties of TMS-OXA 1:1 co-crystal obtained from the different co-crystallization techniques. Co-crystals were prepared by the slow evaporation (SE) and ultrasound assisted co-crystallization from solution (USSC) methods. The tabletability profiles were plotted between compaction forces in the range of 4.98–29.89 kN vs. tensile strength. The tablet tensile strength of TMS in compaction force >14.98 kN had severe capping or lamination. In contrast, the tablet tensile strengths of the TMS-OXA SE and USSC co-crystals were higher and could be easily formed into tablets in all of the compaction forces. It can be concluded that the TMS-OXA co-crystals prepared by the SE and USSC methods have improved mechanical properties of the telmisartan tablet.

Keywords: telmisartan, oxalic acid, co-crystal, slow evaporation, ultrasound assisted co-crystallization from solution

1. Introduction

The most common form of pharmaceutical dosage given to patients is the solid form (tablets and capsules) (Morissette *et al.*, 2004). The design of a pharmaceutical solid material with a favorable the physicochemical properties of drugs is a challenge for the researcher in the pharmaceutical industry, so patients can receive drugs that are safe, effective and inexpensive (Basavoju, Boström, & Velaga, 2008). One of the continuous challenges in the development and manufacture of drugs is the poor mechanical properties. Difficulties often arise during grinding, filling and the compaction process due to the poor mechanical properties of the powder (C. Sun & Grant, 2001).

Telmisartan (TMS) is used for the prevention and treatment of hypertension that is commercially available as Micardis® categorized as an angiotensin II receptor antagonist. Its low solubility and high permeability make this active pharmaceutical ingredient (API) included in a class II in the biopharmaceutical classification system. Three forms of TMS crystals, i.e. one solvate and two polymorphics (forms A and B) were reported by Dinnebier (Dinnebier, Sieger, Nar, Shankland, & David, 2000). The crystal habit may affect the orientation of the particles; therefore, it will cause changes in the properties such as flowability, compression, and dissolution of the APIs. Celecoxib has properties similar to TMS. Celecoxib has cohesive needle-shaped crystals, high

*Corresponding author
Email address: hestiary_ratih@yahoo.co.id

surface energy, and an electric charge which tend to cause agglomeration during mixing that may lead to content non-uniformity during capsule filling operations (Banga, Chawla, Varandani, Mehta, & Bansal, 2007). In a study conducted by Banga (2007), the crystal habit of celecoxib was modified to overcome those manufacturing problems.

Crystal engineering through co-crystal formation is one of the approaches to improve the physicochemical properties of the APIs including solubility and mechanical properties (Almarsson & Zaworotko, 2004). A co-crystal is defined as a material containing two or more different molecules that make up the new crystalline form (Trask & Jones, 2005). The formation of the caffeine-methylgallate co-crystal can modify the powder compactibility of pure caffeine (C. C. Sun & Hou, 2008). The mechanical properties of paracetamol co-crystals with theophylline, oxalic acid, naphthalene, phenazine, and 5-nitro isophthalic acid have better compression compared to paracetamol form I (Hiendrawan *et al.*, 2016; Karki *et al.*, 2009). The formation of a co-crystal depends on the presence of a supramolecular synthon between the API and the coformer. TMS contains two imidazole rings and an aromatic carboxylic acid which causes the TMS to have several hydrogen bond acceptors and hydrogen bond donors (Figure 1). Much research has been conducted on TMS co-crystal formation. In a previous study, the solubility and dissolution rate of TMS increased through the TMS-oxalic acid (OXA) co-crystal formation, and the crystal habit of the TMS-OXA co-crystal was rhomboid-shaped that generally had good mechanical properties when developed into a tablet dosage form (Alatas, Ratih, & Soewandhi, 2015). A continuation of the study on the mechanical properties of the TMS-OXA co-crystal such as flowability and tensile strength was conducted. This study aimed to prepare the TMS-OXA co-crystal by the slow evaporation (SE) method to achieve a larger crystal size. This study also aimed to produce large quantities of co-crystals for scale-up purposes using ultrasound-assisted co-crystallization (USSC) from solution. The purpose of this research was to study the influence of TMS-OXA co-crystals prepared from two co-crystallization techniques (SE and USSC) on the mechanical and compaction properties of TMS.

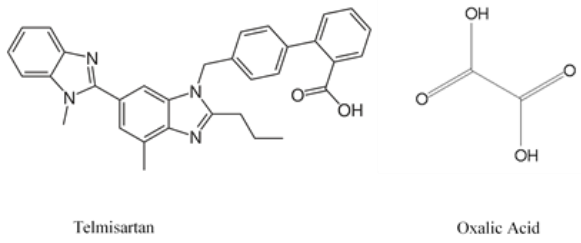

Figure 1. Chemical structure of telmisartan (TMS) and oxalic acid (OXA).

2. Materials and Methods

2.1.1 Materials

TMS with a purity of >99% was purchased from Glenmark Pharmaceutical Limited, Mumbai, India (batch no. 0171200922). Oxalic acid dihydrate (OXA) dihydrate, methanol and other reagents were bought from Merck Chemicals Indonesia.

2.1.2 Methods

1) Telmisartan/oxalic acid 1:1 co-crystal preparation

a. Slow evaporation (SE)

TMS-OXA co-crystals with a 1:1 molar ratio were prepared by the SE method in methanol solvent. Five grams of TMS, 1.22 g of OXA, and 700 mL of methanol were put in a closed Erlenmeyer flask which was placed in a waterbath shaker at about 70 °C until a clear solution was obtained. The solution was then filtered and allowed to evaporate at room temperature until co-crystals were formed. The co-crystals were characterized by powder X-ray diffraction (PXRD), polarization microscope, differential scanning calorimeter (DSC) and Fourier transform infrared (FTIR) spectroscopy.

b. Ultrasound-assisted co-crystallization (USSC) from solution

Ultrasonic / high intensity sonifier (Branson, Model 3510E-DTH, Danbury, USA) operated with 42 kHz vibrations at 40 °C which is able to induce a maximum power output of 100 W. Five grams of TMS and 1.22 g of OXA were placed in a glass beaker with 100 mL of methanol and sonicated for 5–10 minutes. Samples of the solid mixture were taken every one minute and observed under a microscope until rhomboid-shaped crystals were formed. The solid mixture was separated by filtration and dried at ambient temperature. The dried solid was kept in a desiccator until further study.

2) Characterization of co-crystals

a. Powder X-ray diffraction (PXRD)

PXRD was performed using a Philips PW1710 X-ray diffraction system. Data were collected from 5 to 35º 2θ using continuous scanning, with a scan rate of 2º/min. The X-ray tube was operated at 40 kV, 30 mA.

b. Differential scanning calorimetry (DSC)

A 1-3 mg of each sample was tested using the DSC Q20 instrument (TA Instruments, DE, USA) which was calibrated with indium in the range of 50 to 300 ° C and a heating speed of 10 ° C / minute. Nitrogen gas flow at 50 mL / min is used for continuous sample cleaning.

c. Fourier transform infrared (FTIR) spectroscopy

IR spectra of the compounds were recorded on an FTIR Affinity-1 spectrophotometer (DRS-8000) Shimadzu, Japan. Forty-five scans were obtained from 4000 to 400 cm^{-1}.

d. Scanning electron microscopy (SEM)

The morphology of the samples (crystal habit) was examined using SEM (JEOL JSM-6360LA, Japan). Double-sided adhesive tape was used to glue the specimen to a metal

sample holder with a diameter of 12 mm that was coated with palladium gold.

e. Particle size analysis

A Beckman Coulter LS 13 1320 laser diffraction particle analyser equipped with R5 lens with measuring range 0.375-2000 µm was used for the determination of volume-weighed particle size of TMS, TMS-OXA co-crystal SE and USSC.

f. Helium pycnometry

Helium pycnometer (Ultrapycnometer 1000e version 4, Quantachrome Instruments, USA) was used to determine the densities of TMS and TMS-OXA cocrystal SE and USSC. The gas pressure input was 17 psi with one-minute equilibrium time The mean of 3 determinations was reported with standard deviation of 0.05%.

g. Flowability studies

Compressibility and flowability were determined by measuring the bulk density (ρ_b) and tap density (ρ_t). The volume before and after tapping was used to determine ρ_b and ρ_t, respectively. The Carr index and the Hausner ratio were calculated using the equations 1 and 2:

$$\text{Carr index} = \frac{\rho_t - \rho_b}{\rho_t} \times 100\% \quad (1)$$

$$\text{Hausner ratio} = \frac{\rho_b}{\rho_t} \quad (2)$$

h. Powder compaction

Hydraulic press equipment (Perkin Elmer, MA, USA) was used to compress tablets at pressure 4.9-29.4 kN with a 11 mm diameter of punch, each containing about 300 mg of pure TMS powder and TMS-OXA co-crystal produced by SE and USSC. Magnesium stearate is added as a lubricant for each compression. Compressed tablets were measured in diameter and thickness using thickness gaus (Mitutoyo, Japan), while the hardness was measured by a hardness tester (Type PTB 111, Pharma Test, Germany). Breaking force, tablet diameter, and tablet thickness data was used to compute the tensile strength (σ) according to Equation 3.

$$\sigma = \frac{2F}{\pi DT} \quad (3)$$

where F is the breaking force (Newtons), D is the tablet diameter (mm), and T is the thickness of the tablet (mm).

Elastic recovery (ER) depends on the amount of elastic energy stored during and after the compression process and it can be calculated based on the diameter before (Ho) and after (H) storage for 24 hours, as shown in equation 4 (Sun and Grant, 2001):

$$\%\,ER = \frac{H - H_o}{H_o} \times 100 \quad (4)$$

i. *In-vitro* dissolution test

A 900 mL buffer pH 7.5 phosphate solution was used as a dissolution medium for each of the TMS and TMS-OXA co-crystals of SE and USSC. Each dissolution test was carried out for 60 minutes using a type 2 device (ZRS-6G, Tianjin, China). 40 mg TMS and TMS-OXA co-crystal (SE and USSC) equivalent to 40 mg TMS were added, and a 10 mL aliquot was withdrawn at different intervals and filtered using a 0.45 µm membrane filter. The drug concentration was analyzed using a Shimadzu 1601-PC spectrophotometer at a wavelength of 295 nm.

3. Results and Discussion

PXRD is a reliable technique for indicating the formation of new solid phase. The product obtained after the process of co-crystallization showed a different PXRD pattern of the individual components which confirmed the formation of a new crystalline phase (Goud, Suresh, Sanphui, & Nangia, 2012; Hiendrawan *et al.*, 2016). The PXRD pattern for TMS, OXA, and TMS-OXA co-crystal prepared by SE and USSC are shown in Figure 2. TMS showed characteristic crystalline peaks at 2θ values of 6.79, 14.21, 15.02, 19.10, 21.36, 22.33, and 25.07°, while OXA showed characteristic crystalline peaks at 2θ values of 14.75, 29.00, and 31.53°. The main peaks of TMS and OXA disappear and new peaks appear on the formation of TMS-OXA co-crystals which indicate the formation of a new crystalline phase. The main peaks of the co-crystal TMS-OXA (1:1) are located at 2θ with values of 7.06, 7.54, 11.79, 12.98, 13.46, 14.86, 16.2, 16.5, 18.35, 21.64, 22.93, 23.67, 24.96, and 27.06°. The PXRD pattern of the co-crystal prepared by SE and USSC showed no difference. The PXRD spectra showed that the product produced by USSC method has a lower crystallinity than the SE method. In the SE method, the process of co-crystal recrystallization was so slow that the crystals took a longer time to form larger crystals which resulted in higher crystallinity than the co-crystals produced by the USSC method.

DSC experiments were conducted to determine the thermal behavior of the TMS, OXA, TMS-OXA SE and USSC co-crystals (Figure 3). The TMS-OXA SE and USSC co-crystals melted at a temperature of 230.7 ℃ and 231.5 ℃, respectively. The melting points of the co-crystals were between the TMS and OXA melting points which showed their physical interaction to produce co-crystals.

FTIR is a reliable general spectroscopic technique that is used in addition to determining the chemical conformation of compounds as well as to detect the formation of co-crystals, especially when using carboxylic acids as coformers and/or when an acid and a base form a neutral O-H—N hydrogen bond (Qiao *et al.*, 2011; Schultheiss & Newman, 2009). This interaction can be detected by the presence of vibrational frequency changes of the functional groups (Aitipamula, Wong, Chow, & Tan, 2014; Chadha, Saini, Jain, & Venugopalan, 2012). The FTIR spectrum of the co-crystals obtained by SE and USSC are shown in Figure 4. The FTIR spectrum of TMS showed peaks at 3059, 2958, 1695, and 1603 cm^{-1}, which corresponded to the aromatic –CH stretch, aliphatic –CH stretch, –C=O stretch, and imine

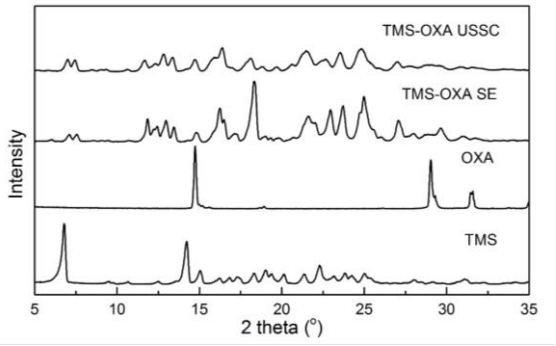

Figure 2. Powder X-ray diffractograms of TMS-OXA co-crystal prepared by slow evaporation (SE) and ultrasound-assisted co-crystallization (USSC) from solution compared to its starting components.

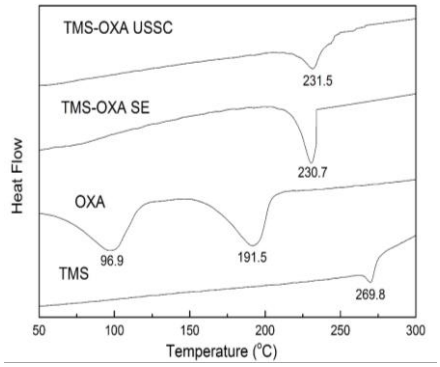

Figure 3. DSC thermograms of TMS-OXA co-crystals prepared by slow evaporation (SE) and ultrasound-assisted co-crystallization (USSC) from solution compared to the starting components.

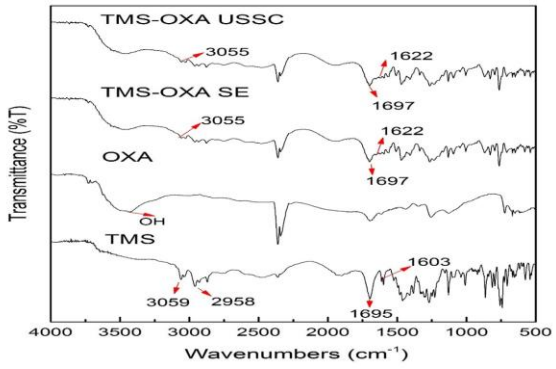

Figure 4. FTIR spectra of TMS-OXA SE and USSC co-crystals compared to the starting components.

C=N stretch, respectively. An increase in the –C=O stretch frequency of TMS from 1695 cm^{-1} to 1697 cm^{-1} and C=N stretch from 1603 cm^{-1} to 1622 cm^{-1} in the TMS-OXA SE and USSC implied supramolecular heterosynthon formation of the co-crystals (Alatas *et al.*, 2015). The FTIR spectrum of the TMS-OXA co-crystals obtained from the SE and USSC methods showed the same peaks and did not show a different spectrum.

SEM images of co-crystals obtained by SE and USSC are shown in Figure 5. In both cases, rhomboid shape crystal habit was observed. Some studies have described that more regular shape crystal habit makes more free flowing powder and has good tabletability properties. Paracetamol polyhedral crystals produce tablets that are stronger than untreated paracetamol crystals (Kaialy, Larhrib, Chikwanha, Shojaee, & Nokhodchi, 2014). Orthorombic paracetamol shows better tabletability than the monoclinic form (Joiris *et al.*, 1998). Co-crystals obtained from SE method has a wide particle size range from 20-170 µm. This size variation resulted from the slow removal of solvent along with the decreasing temperature of the solution so that the crystal may grow well. On the other hand, USSC product produced crystals in a much narrower size range (5-20 pm) than the SE method. USSC co-crystals were in the form of rhomboid shape crystals agglomerates (Figure 5d). The USSC method has the advantage of being producing small size particles in a narrow size range using a single step process, whereas SE crystals need to be further milled in order to obtain uniform small size (Aher, Dhumal, Mahadik, Paradkar, & York, 2010). During the application of ultrasound for USSC solution, the nucleation of the particles free solution is influenced by the presence of ultrasonic wave cavitation energy. The primary nucleation at lower saturation level can be induced by the phenomenon of cavitation by reducing the induction period and the width of metastable zones (Li, Li, Guo, & Liu, 2006; Luque de Castro & Priego-Capote, 2007; Ruecroft, Hipkiss, Ly, Maxted, & Cains, 2005). Therefore, in the USSC method, a growing number of primary nuclei are formed and ultimately present finer and more uniform particles than SE method which provides uncontrolled nucleation and crystal growth environments resulting in a wide particle size distribution (Aher *et al.*, 2010).

The micromeritic properties such as flowability of the co-crystals and pure drug are shown in Table 1. Pure TMS has a lower tapped density than the TMS-OXA co-crystal (SE and USSC methods). This could be attributed to the presence of internal friction among the TMS particles that was high enough so that a lot of empty space was not filled because of the needle-shaped TMS habit. From the result of the Carr index and Hausner ratio, it was found that co-crystals (SE & USSC) had better flowability than that of pure TMS. The high

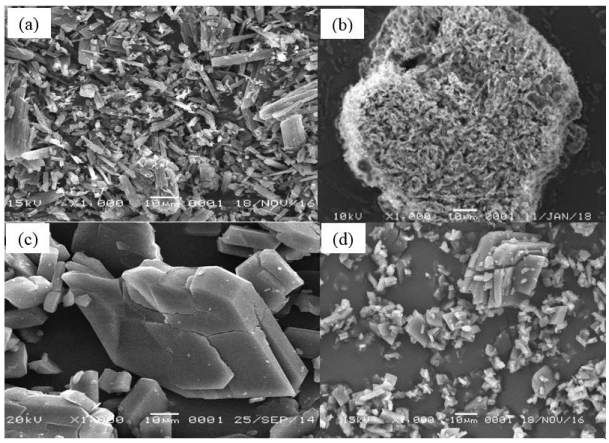

Figure 5. SEM images of (a) TMS, (b) OXA, (c) TMS-OXA SE co-crystals, and (d) TMS-OXA USSC co-crystals.

Table 1. Physical properties of TMS, TMS-OXA SE and USSC co-crystals.

Sample	Tapped density	True density	Carr index (%)	Hausner ratio	Flow character
TMS	0.223±0.003	1.394±0.004	36.4±2.53	1.57±0.31	Poor
TMS-OXA SE	0.754±0.007	1.425±0.007	13.8±2.19	1.16±0.99	Good
TMS-OXA USSC	0.521±0.006	1.755±0.008	17.9±2.25	1.21±0.12	Fair

flowability of co-crystals compared to TMS might result from the decreasing cohesiveness of co-crystals. Less irregular degradation of the TMS-OXA co-crystal habit compared to TMS crystal habit resulted in a decrease in the contact area of the particles, leading to decreased cohesion properties among particles (Kaialy *et al.*, 2014). This could be confirmed by the crystal morphological analysis of the SEM analysis is shown in Figure 5. TMS-OXA co-crystal (USSC) has a lower flowability than TMS-OXA co-crystal (SE). In general, particles of smaller size tend to be more cohesive and thus have lower flowability than those of larger particle sizes (Kaialy, Larhrib, Ticehurst, & Nokhodchi, 2012).

The high Carr index value in TMS (Table 1) may have resulted from powder aggregation due to the high level of mechanical interlocking among molecules in the needle-shaped of TMS crystals (Figure 5a). On the other hand, the decreased CI values for TMS-OXA co-crystal (SE and USSC) might result from the relatively decreased inter-particle contact areas so that the cohesion decreased compared to TMS which resulted in fewer points of physical contact and higher true density (Kaialy *et al.*, 2014).

The flowability and tabletability are the important factors in tablet manufacturability of a powder. Tabletability is defined as the ability of a powder to be compressed into tablets with specific strength at a certain pressure (Jain, Khomane, & Bansal, 2014). Figure 6 shows the tabletability plot for TMS, TMS-OXA SE and USSC co-crystal. The tabletability profiles were measured by a compaction pressure range of 4.98 to 29.89 kN. TMS can be compressed at the range of 4.98 - 14.98 kN but if the compaction force is above 14.98 kN, the TMS would have a brittle or fracture. It can be seen in the capping on TMS tablets above 14.98 kN pressure so that the tensile strength cannot be measured.

According to Dinnebier, TMS form A consisted of a needle-shaped crystal habit that had some unfavorable properties for the drug manufacturing process due to high electrostatic forces, poor flowability, and low density. These properties resulted in the TMS particles experiencing high internal friction or cohesiveness that led to a lot of empty space on the die that was not filled during the compaction process. Consequently, some air entrapment in the die resulted in capping (Dinnebier *et al.*, 2000; Kaialy *et al.*, 2014). In contrast, the tablet tensile strength of TMS-OXA SE and USSC co-crystals could be formed in tablets in all of the compaction forces. The TMS-OXA USSC co-crystals had a higher tensile strength value compared with the TMS-OXA SE co-crystals which indicated that the TMS-OXA USSC co-crystal tabletability was better than the TMS-OXA SE co-crystals. At the lowest compaction pressure of 4.8 kN, the TMS-OXA USSC co-crystals yielded a tensile strength of 2.22 MPa which increased continuously to 2.98 MPa at a compaction pressure of 29.89 kN. The tensile strength of the tablet must reach 2 MPa in order to form a good tablet for production (Perumalla & Sun, 2014). The TMS-OXA USSC

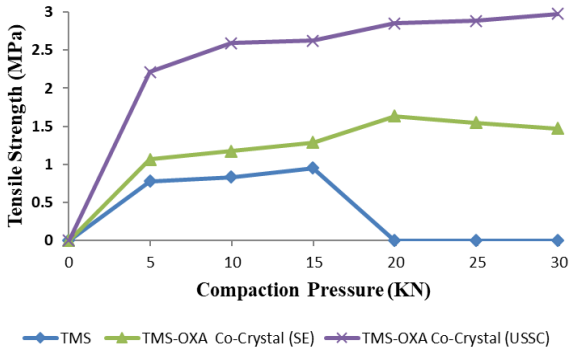

Figure 6. Tabletability profiles of TMS, TMS-OXA SE and USSC co-crystals.

co-crystals met these criteria and in manufacturing there should be no problem in tabletability. There was no tendency of capping or lamination in the TMS-OXA USSC co-crystal tablets (Figure 7). The tensile strength of TMS-OXA SE co-crystals only reached 1.64 Mpa at a compaction force of 19.93 kN, but the results were better than pure TMS which had a capping or lamination tendency at >14.98 kN. In general, the ability of powder compaction with smaller particle sizes is better than larger particle sized powders due to the increased surface area of the powder with small particle sizes that exhibit better bonding compared to larger particle size powders. The results showed that the TMS-OXA USSC co-crystal powder had smaller particle sizes compared to the TMS-OXA SE co-crystal powder (Table 2). Therefore, the tablet tensile strength of the TMS-OXA USSC co-crystal was better than the TMS-OXA SE (Hiendrawan *et al.*, 2016; C. Sun & Grant, 2001).

The compaction properties of bulk viscoelastic materials were determined by the relative excellence of elastic and plastic deformation constituents. As a result of the rearrangement and deformation of particles under mechanical stress during the powder compaction process, a developing area of bonding between particles develops. The area of inter-particle bonding is maintained in sufficient quantities after the loss of compaction pressure and the release of the tablet from the die caused the formation of intact tablet. Therefore, materials with low plasticity show poor powder compaction properties due to the difficulty in forming sufficient bonding areas after compaction (Chattoraj *et al.*, 2014). TMS tablets at compaction pressure >14.98 kN could not be determined due to the capping/lamination when the tablet is ejected out of the die, so that the elastic recovery cannot be measured. It was clear that the plasticity of TMS crystal was low as supported by the relative high elastic recovery (ER) of TMS during decompression, e.g., ± 0.95 % at 14.98 kN (Figure 8). Based on the result of tabletability profile and % elastic recovery, as a result of the level of interparticulate bonding (bond area and

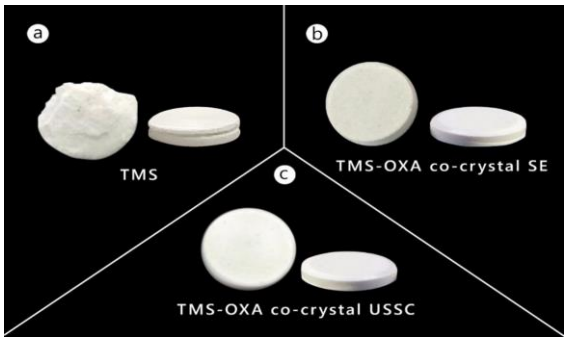

Figure 7. Tablet overview of a) TMS capping, b) TMS-OXA SE co-crystal, c) TMS-OXA USSC co-crystals at a compaction force of 19.98 kN.

Table 2. Particle size distribution for TMS, TMS-OXA SE and USSC co-crystals.

Particle size distribution	TMS	TMS-OXA SE co-crystal	TMS-OXA USSC co-crystal
d_{10} (μm)	0.928	1.307	0.493
d_{50} (μm)	4.180	5.852	1.598
d_{90} (μm)	11.24	11.8	2.185

bond strength), the plasticity of the TMS-OXA co-crystal SE and USSC was higher than TMS. This implied that the co-crystal has a low porosity and a stronger tablet at the same compaction pressure compared to TMS (Aher, Dhumal, Mahadik, Ketolainen, & Paradkar, 2011). Several reports also show that the greater plasticity which affects the harder tablet was caused by the slip plane on the crystal lattice (Jain *et al.*, 2014; C. C. Sun & Hou, 2008). Further research should be conducted to investigate the crystal structure of TMS and TMS-OXA and its relationship with tablet properties improvement.

In addition, the co-crystals obtained from the two different techniques (SE and USSC) exhibited the same habit (rhomboid shape), but the different elastic properties of the crystals showed different compaction properties which need to be studied further in different co-crystallization techniques. It has been previously demonstrated that the USSC application in crystallization showed morphological changes such as crystal surface properties which included particle size, flowability and elastic properties, and different properties compared to slow evaporation resulting in very different compaction behavior (Aher *et al.*, 2011; Amara, Ratsimba, Wilhelm, & Delmas, 2001; Dhumal, Biradar, Paradkar, & York, 2008; Guo, Zhang, Li, Wang, & Kougoulos, 2005).

Besides the mechanical properties, dissolution is also essential to formulate a solid dosage oral form as it is closely connected with bioavailability. The profile of powder dissolution for the release of TMS from the pure drug and co-crystals (SE and USSC) in pH 7.5 phosphate buffer are shown in Figure 9. The dissolution rate showed that the dissolution percentages of TMS at 60 min of the TMS-OXA SE and USSC co-crystals were higher than the pure TMS. The dissolution percentages at 60 min of pure TMS, TMS-OXA SE, and TMS-OXA USSC were 7.7%, 55.7%, and 59.9%, respectively.

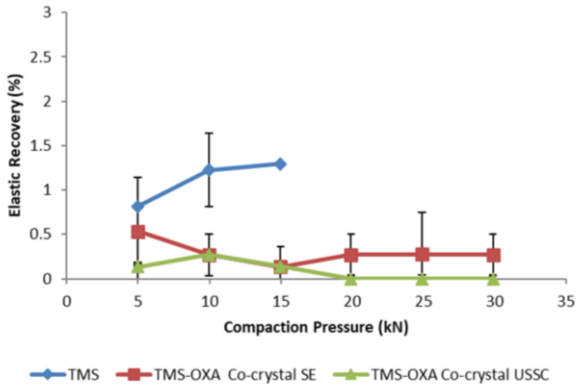

Figure 8. Elastic recovery of TMS, TMS-OXA SE and USSC co-crystals.

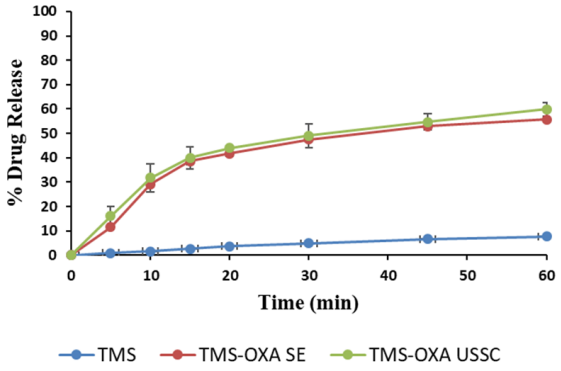

Figure 9. Dissolution profile of TMS, TMS-OXA SE and USSC co-crystals in phosphate buffer pH 7.5.

4. Conclusions

Co-crystal formations between TMS with OXA were prepared by the SE and USSC methods. Characterization of the co-crystals included PXRD, DSC, FTIR, and SEM. The formation of TMS-OXA co-crystals by the SE and USSC methods improved the mechanical properties and produced a better tableting performance compared to pure TMS. Co-crystals obtained by the two co-crystallization techniques showed a similar crystal habit, but they had different mechanical properties. Therefore, the crystal surface properties need to be studied further to understand the differences in compacting behavior as well as investigating the crystal structure of TMS and TMS-OXA and its relationship with tablet property improvement. The dissolution profile of the TMS-OXA co-crystals can increase the dissolution rate of TMS. The results of this study offer a better approach to improve the mechanical properties and dissolution of TMS by co-crystallization with OXA.

Acknowledgements

We would like to thank the Directorate General of Higher Education, Indonesia Ministry of Education and Culture for the doctoral educational program scholarship.

References

Aher, S., Dhumal, R., Mahadik, K., Ketolainen, J., & Parad kar, A. (2011). Effect of cocrystallization techniques on compressional properties of caffeine/oxalic acid 2:1 cocrystal. *Pharmaceutical Development and Technology*, *18*(June 2011), 1–6. doi:10.3109/10837450.2011.618950

Aher, S., Dhumal, R., Mahadik, K., Paradkar, A., & York, P. (2010). Ultrasound assisted cocrystallization from solution (USSC) containing a non-congruently soluble cocrystal component pair: Caffeine/maleic acid. *European Journal of Pharmaceutical Sciences*, *41*(5), 597–602. doi:10.1016/j.ejps.2010.08.012

Aitipamula, S., Wong, A. B. H., Chow, P. S., & Tan, R. B. H. (2014). Pharmaceutical salts of haloperidol with some carboxylic acids and artificial sweeteners: Hydrate formation, polymorphism, and physicochemical properties. *Crystal Growth and Design*, *14*(5), 2542-2556. doi:10.1021/cg500245e

Alatas, F., Ratih, H., & Soewandhi, S. N. (2015). Enhancement of solubility and dissolution rate of telmisartan by telmisartan-oxalic acid co-crystal formation. *International Journal of Pharmacy and Pharmaceutical Sciences*, *7*(3), 423–426.

Almarsson, Orn, & Zaworotko, M. J. (2004). Crystal engineering of the composition of pharmaceutical phases. Do pharmaceutical co-crystals represent a new path to improved medicines? *Chemical Communications*, *17*, 1889. doi:10.1039/b402150a

Amara, N., Ratsimba, B., Wilhelm, A. M., & Delmas, H. (2001). Crystallization of potash alum: Effect of power ultrasound. *Ultrasonics Sonochemistry*, *8*(3), 265–270. doi:10.1016/S1350-4177(01)00087-6

Banga, S., Chawla, G., Varandani, D., Mehta, B. R., & Bansal, A. K. (2007). Modification of the crystal habit of celecoxib for improved processability. *The Journal of Pharmacy and Pharmacology*, *59*(1), 29–39. doi:10.1211/jpp.59.1.0005

Basavoju, S., Boström, D., & Velaga, S. P. (2008). Indomethacin-saccharin cocrystal: Design, synthesis and preliminary pharmaceutical characterization. *Pharmaceutical Research*, *25*(3), 530–541. doi:10.1007/s11095-007-9394-1

Chadha, R., Saini, A., Jain, D. S., & Venugopalan, P. (2012). Preparation and solid-state characterization of three novel multicomponent solid forms of oxcarbazepine: Improvement in solubility through saccharin cocrystal. *Crystal Growth and Design*, *12*(8), 4211–4224. doi:10.1021/cg3007102

Chattoraj, S., Shi, L., Chen, M., Alhalaweh, A., Velaga, S., & Sun, C. C. (2014). Origin of deteriorated crystal plasticity and compaction properties of a 1:1 cocrystal between piroxicam and saccharin. *Crystal Growth and Design*, *14*(8), 3864–3874. doi:10.1021/cg500388s

Dhumal, R. S., Biradar, S. V., Paradkar, A. R., & York, P. (2008). Ultrasound assisted engineering of lactose crystals. *Pharmaceutical Research*, *25*(12), 2835–2844. doi:10.1007/s11095-008-9653-9

Dinnebier, R. E., Sieger, P., Nar, H., Shankland, K., & David, W. I. F. (2000). Structural characterization of three crystalline modifications of telmisartan by single crystal and high-resolution X-ray powder diffraction. *Journal of Pharmaceutical Sciences*, *89*(11), 1465–1479. doi:10.1002/1520-6017(200011)89:11<1465::AID-JPS9>3.0.CO;2-C

Goud, N. R., Suresh, K., Sanphui, P., & Nangia, A. (2012). Fast dissolving eutectic compositions of curcumin. *International Journal of Pharmaceutics*, *439*(1–2), 63–72. doi:10.1016/j.ijpharm.2012.09.045

Guo, Z., Zhang, M., Li, H., Wang, J., & Kougoulos, E. (2005). Effect of ultrasound on anti-solvent crystallization process. *Journal of Crystal Growth*, *273*(3–4), 555–563. doi:10.1016/j.jcrysgro.2004.09.049

Hiendrawan, S., Veriansyah, B., Widjojokusumo, E., Soewandhi, S. N., Wikarsa, S., & Tjandrawinata, R. R. (2016). Physicochemical and mechanical properties of paracetamol cocrystal with 5-nitroisophthalic acid. *International Journal of Pharmaceutics*, *497*(1–2), 106–113. doi:10.1016/j.ijpharm.2015.12. 001

Jain, H., Khomane, K. S., & Bansal, A. K. (2014). Implication of microstructure on the mechanical behaviour of an aspirin–paracetamol eutectic mixture. *CrystEng Comm*, *16*(36), 8471–8478. doi:10.1039/x0xx00000x

Joiris, E., Di Martino, P., Berneron, C., Guyot-Hermann, A.-M., & Guyot, J.-C. (1998). Compressive Behaviour of Orthorhombic Paracetamol. *Pharmaceutical Research*, *15*(7), 1122–1130. doi:10.1023/A:1011954800246

Kaialy, W., Larhrib, H., Chikwanha, B., Shojaee, S., & Nokhodchi, A. (2014). An approach to engineer paracetamol crystals by antisolvent crystallization technique in presence of various additives for direct compression. *International Journal of Pharmaceutics*, *464*(1–2), 53–64. doi:10.1016/j.ijpharm.2014.01.026

Kaialy, W., Larhrib, H., Ticehurst, M., & Nokhodchi, A. (2012). Influence of batch cooling crystallization on mannitol physical properties and drug dispersion from dry powder inhalers. *Crystal Growth and Design*, *12*(6), 3006–3017. doi:10.1021/cg300224w

Karki, S., Friščić, T., Fabián, L., Laity, P. R., Day, G. M., & Jones, W. (2009). Improving mechanical properties of crystalline solids by cocrystal formation: new compressible forms of paracetamol. *Advanced Materials*, *21*(38–39), 3905–3909. doi:10.1002/adma.200900533

Li, H., Li, H., Guo, Z., & Liu, Y. (2006). The application of power ultrasound to reaction crystallization. *Ultrasonics Sonochemistry*, *13*(4), 359–363. doi:10.1016/j.ultsonch.2006.01.002

Luque de Castro, M. D., & Priego-Capote, F. (2007). Ultrasound-assisted crystallization (sonocrystallization). *Ultrasonics Sonochemistry*, *14*(6), 717–724. doi:10.1016/j.ultsonch.2006.12.004

Morissette, S. L., Almarsson, Ö., Peterson, M. L., Remenar, J. F., Read, M. J., Lemmo, A. V., Gardner, C. R. (2004). High-throughput crystallization: Poly-

morphs, salts, co-crystals and solvates of pharmaceutical solids. *Advanced Drug Delivery Reviews*, *56*(3), 275–300. doi:10.1016/j.addr.2003.10.020

Perumalla, S. R., & Sun, C. C. (2014). Enabling tablet product development of 5-fluorocytosine through integrated crystal and particle engineering. *Journal of Pharmaceutical Sciences*, *103*(4), 1126–1132. doi:10.1002/jps.23876

Qiao, N., Li, M., Schlindwein, W., Malek, N., Davies, A., & Trappitt, G. (2011). Pharmaceutical cocrystals: An overview. *International Journal of Pharmaceutics*, *419*(1–2), 1–11. doi:10.1016/j.ijpharm.2011.07.037

Ruecroft, G., Hipkiss, D., Ly, T., Maxted, N., & Cains, P. W. (2005). Sonocrystallization: The use of ultrasound for improved industrial crystallization. *Organic Process Research and Development*, *9*(6), 923–932. doi:10.1021/op050109x

Schultheiss, N., & Newman, A. (2009). Pharmaceutical cocrystals and their physicochemical properties. *Crystal Growth and Design*, *9*(6), 2950–2967. doi:10.1021/cg900129f

Sun, C. C., & Hou, H. (2008). Improving Mechanical Properties of Caffeine and Methyl Gallate Crystals by Cocrystallization Improving Mechanical Properties of Caffeine and Methyl Gallate Crystals by Cocrystallization. *Crystal Growth and Design*, (Scheme 1). doi:10.1021/cg700843s

Sun, C., & Grant, D. (2001). Effects of initial particle size on the tableting properties of L-lysine monohydrochloride dihydrate powder. *International Journal of Pharmaceutics*, *215*(1–2), 221–228. doi:10.1016/S0378-5173(00)00701-8

Trask, A. V, & Jones, W. (2005). Crystal engineering of organic cocrystals by the solid-state grinding approach. In Toda F. (Ed.), *Organic solid state reactions. Topics in current chemistry* (pp. 41–70). Heidelberg, Germany: Springer. doi:10.1007/b100995.